The p53 cofactor Strap exhibits an unexpected TPR motif and oligonucleotide-binding (OB)–fold structure

Cassandra J. Adams[a,1], Ashley C. W. Pike[b,1], Sandra Maniam[a], Timothy D. Sharpe[b], Amanda S. Coutts[a], Stefan Knapp[b], Nicholas B. La Thangue[a,2], and Alex N. Bullock[b,2]

[a]Laboratory of Cancer Biology, Department of Oncology, Medical Sciences Division, University of Oxford, Old Road Campus Research Building, Roosevelt Drive, Oxford, OX3 7DQ, United Kingdom; and [b]Structural Genomics Consortium, Nuffield Department of Clinical Medicine, University of Oxford, Old Road Campus Research Building, Roosevelt Drive, Oxford, OX3 7DQ, United Kingdom

Edited by Alan R. Fersht, MRC Laboratory of Molecular Biology, Cambridge, United Kingdom, and approved January 17, 2012 (received for review August 23, 2011)

Activation of p53 target genes for tumor suppression depends on the stress-specific regulation of transcriptional coactivator complexes. Strap (stress-responsive activator of p300) is activated upon DNA damage by ataxia telangiectasia mutated (ATM) and Chk2 kinases and is a key regulator of the p53 response. In addition to antagonizing Mdm2, Strap facilitates the recruitment of p53 coactivators, including JMY and p300. Strap is a predicted TPR-repeat protein, but shows only limited sequence identity with any protein of known structure. To address this and to elucidate the molecular mechanism of Strap activity we determined the crystal structure of the full-length protein at 2.05 Å resolution. The structure of Strap reveals an atypical six tetratricopeptide repeat (TPR) protein that also contains an unexpected oligonucleotide/oligosaccharide-binding (OB)-fold domain. This previously unseen domain organization provides an extended superhelical scaffold allowing for protein-protein as well as protein-DNA interaction. We show that both of the TPR and OB-fold domains localize to the chromatin of p53 target genes and exhibit intrinsic regulatory activity necessary for the Strap-dependent p53 response.

crystal | DNA damage | p300 | stress | tumor suppressor

Tumor suppressor p53 is a stress-inducible transcription factor that plays a pivotal role in the prevention of malignant disease (1). The activation of p53 is tightly regulated to effect a variety of cellular outcomes including cell cycle arrest and apoptosis (2). In normal unperturbed cells, p53 levels are kept low by the oncoprotein Mdm2 (3, 4). Under conditions of stress, p53 is stabilized and a plethora of p53 cofactors are recruited to direct the functional p53 response (5).

Strap is a p53 cofactor that interacts with p300 coactivator proteins, and thereby contributes to p53-dependent transcriptional activity (6). In addition, Strap augments the p53 response by downregulating the activity of Mdm2 (6). Strap is stabilized in DNA-damaged cells and accumulates in the nucleus as a result of phosphorylation by the DNA damage responsive protein kinases ATM and Chk2 (7, 8). Nuclear Strap promotes the assembly of a stress-responsive p53 coactivator complex, which includes the coactivators JMY and p300 (6, 9, 10), as well as the arginine methyltransferase PRMT5 which controls the target gene specificity of p53 (11). A variety of studies support the importance of Strap in delivering an effective stress response (6–8, 12).

Strap (also known as tetratricopeptide repeat protein 5, TTC5) has been predicted to be a TPR-repeat protein, but contains in its C-terminus a large region of unknown structure and function. There is consequently a need for structural models to better define functional domains and the molecular mechanisms of its regulation. To address this, we determined the structure of the full-length protein at 2.05 Å resolution. The crystal structure reveals a superhelical TPR-repeat domain and an unpredicted OB-fold domain. The two domains are associated closely in an elongated superhelical fold. We show that both of the TPR and OB domains in Strap are necessary to achieve a p53 response.

Results

Strap Exhibits a Unique TPR Motif OB-fold Structure. The structure of full-length murine Strap was determined using selenomethionine incorporation and single-wavelength anomalous diffraction. The model was refined at 2.05 Å resolution (Table S1). The refined model revealed that Strap adopts an elongated monomeric structure composed of two domains: a 250-residue N-terminal all α-helical domain comprising six tandem TPR motifs and a 125-residue C-terminal all β-sheet oligonucleotide/oligosaccharide-binding (OB)-fold (Fig. 1*A* and *B* and Fig. S1). The domains are connected by a linker region containing a TPR-capping helix (H7) and a small perpendicular helix (H8).

The six TPR motifs assemble into a right-handed superhelical structure that is approximately 60 Å long × 40 Å wide with an enclosed inner channel 40 Å long and 7–15 Å in diameter (Fig. 1 *B* and *C*). The archetypal TPR motif consists of 34 residues that assemble into a pair of antiparallel α-helices (A and B) connected by a short loop (13). TPRs 2, 3, 5 and TPR6 conform to typical TPR motifs with helices of similar length (11–14 residues), whereas TPR1 and TPR4 are nonstandard motifs. TPR1 is unusually elongated, spanning 61 residues, with component helices nearly twice as long as standard (20–28 residues) (Table 1 and Fig. S2). The connecting region between TPR1 helix 1A and 1B (residues 29–41) contains short α-and 3_{10} helices. This atypical insert extends across the superhelical axis towards TPR6 and encloses the TPR binding groove. TPR4 is atypical in that its component helices are of unequal length with the B helix twice as long as the A helix (Table 1).

The TPR domain sits atop the OB-fold with TPR6 binding into the concave upper surface of the OB domain, resulting in a considerable interface between the two domains (contact area excluding linker helix is 530 $Å^2$). The presence of the OB-fold was completely unexpected and not predicted by sequence analysis. The sequence signature of this domain is present in all known Straps (from humans to *C. elegans*, Fig. S3) and to our knowledge represents an unique occurrence of a TPR-OB domain fusion.

Author contributions: C.J.A., A.C.W.P., S.M., A.S.C., S.K., N.B.L.T., and A.N.B. designed research; C.J.A., A.C.W.P., S.M., T.D.S., and A.N.B. performed research; C.J.A., A.C.W.P., S.M., T.D.S., A.S.C., S.K., N.B.L.T., and A.N.B. analyzed data; and C.J.A., A.C.W.P., S.M., A.S.C., S.K., N.B.L.T., and A.N.B. wrote the paper.

The authors declare no conflict of interest.

This article is a PNAS Direct Submission.

Freely available online through the PNAS open access option.

Data deposition: The atomic coordinates and structure factors have been deposited in the Protein Data Bank, www.pdb.org [PDB ID codes 4ABN (mouse Strap) and 2XVS (human Strap OB-fold)].

[1]C.J.A. and A.C.W.P. contributed equally to this work.

[2]To whom correspondence may be addressed. E-mail: alex.bullock@sgc.ox.ac.uk or nick.lathangue@oncology.ox.ac.uk.

This article contains supporting information online at www.pnas.org/lookup/suppl/doi:10.1073/pnas.1113731109/-/DCSupplemental.

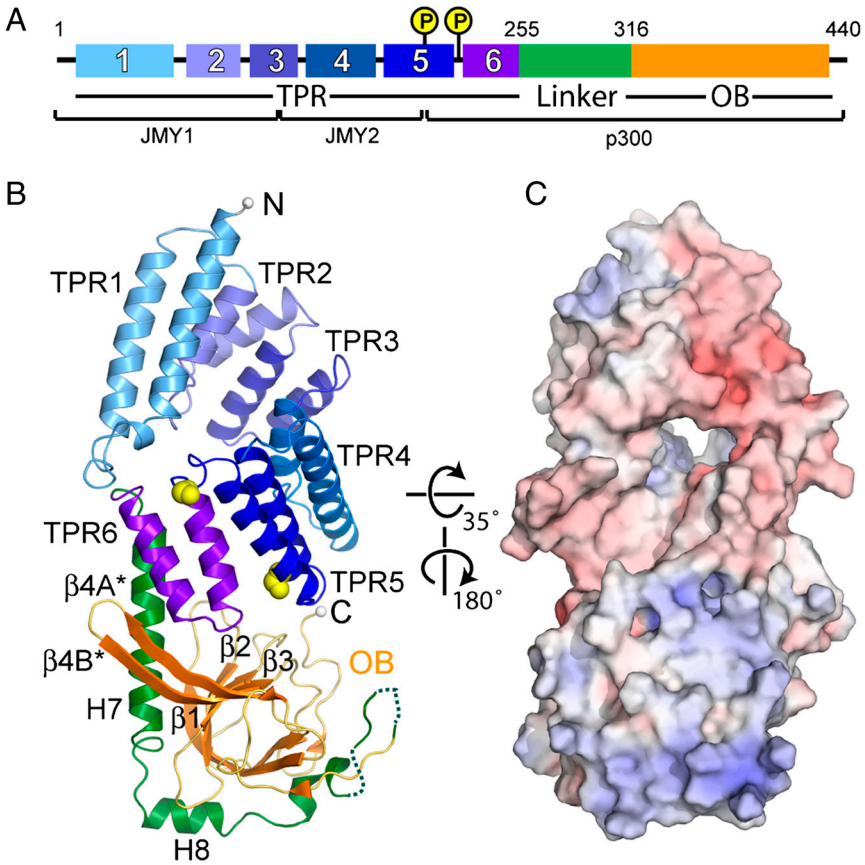

Fig. 1. Overview of the Strap structure. (*A*) Domain organization showing mapped interactions for JMY (two sites labeled JMY1 and JMY2) and p300 (6). Reported phosphorylation sites (7, 8) are highlighted by yellow spheres. (*B*) Ribbon diagram with secondary structure elements colored as in *A*. Reported phosphorylation sites are highlighted by small yellow spheres. (*C*) Surface representation colored by electrostatic potential between −10 and +10 kT.

Strap is a Scaffold Protein for Protein-Protein Interactions. TPR proteins are known to provide a scaffold for the assembly of multiprotein complexes and exhibit a characteristic binding groove, or channel, on the concave surface of the TPR repeat (13). To explore this idea in the context of Strap, we mapped onto the structure the previously identified interaction domains for the p53 coactivators JMY and p300 (Fig. 2*A*). JMY binding was mapped previously by coprecipitation to two domains in Strap (residues 1–123 and 123–205) (6). The structural model revealed these domains to be congruent parts of the TPR channel, representing the upper (TPR1-3) and lower (TPR4-5) portions. Here, the inner groove was identified as a site of sequence conservation (Fig. S3) and shared similar dimensions to the TPR scaffold of APC6 bound to CDC26 (Fig. 2*B*) (14), suggesting that Strap can accommodate peptides of similar size (Strap and APC6 superimposed with a rmsd of 2.8 Å for 202 Cα atoms; distance alignment matrix method (DALI) Z-score 16.7 (15)).

The OB-fold displays a highly electropositive surface (Fig. 1*C*) and is most similar to the nucleic acid-binding OB subclass (16).

Table 1. Structural characteristics of the Strap TPR motifs

TPR	Helix A	Length (residues)	Helix B	Length (residues)	Total length (residues)
1	7–28 (1–28)*	22 (28)	42–61	20	61
2	68–78	11	86–98	13	31
3	103–116	14	119–130	12	28
4	136–146	11	154–174	21	39
5	179–195	17	200–216	17	38
6	224–236	13	240–253	14	30

*Values in parentheses refer to Molecule B.

Preliminary biophysical experiments confirm that Strap binds single-stranded and double-stranded DNA in the micromolar range (Fig. S4). The OB-fold is also recognized for mediating protein-protein interactions (16). The p300-binding domain (6) mapped to a C-terminal region of Strap encompassing TPR6 and the OB-fold (residues 206–440; Fig. 2*A*). Here, the OB domain contributed to the lower jaw of the TPR channel and is therefore likely to bring p300 into close proximity with the TPR-bound coactivator JMY. The structure revealed that the canonical OB-fold ligand-binding surface, centered on strands β2 and β3, was occupied by TPR6 and the TPR-capping helix H7 (Fig. 2*C*). The most closely matched OB-fold structure identified by a DALI structural similarity search was the minichromosome maintenance complex (MCM) (17) (PDB 1LTL; rmsd 2.6 Å for 90 Cα atoms; DALI Z-score 9.8). The OB-fold of MCM had this β2-β3 face similarly occluded, but formed additional intramolecular protein-protein interactions through other OB surface regions (Fig. 2*C*). Potentially, these may also contribute to intermolecular Strap interactions.

We further mapped the two reported phosphorylation sites to the interface of TPR5-TPR6 (Fig. 3). The ATM site at S203 (7) was located within the N-terminal region of α5B (TPR5). This side chain was completely buried in the structure and formed hydrogen bonds to E237 (α6A). The Chk2 site at S221 (8) was also partially buried in a 3_{10} helix between TPR5 and TPR6. Phosphorylation of these residues would likely induce electrostatic and steric clashes to perturb the hydrogen bonding network between TPRs 5 and 6, potentially widening out the TPR channel for protein interaction.

To explore the dynamics of this protein in solution we cloned the phospho-mimic double mutant of Strap (S203D/S221D) for

BIOCHEMISTRY

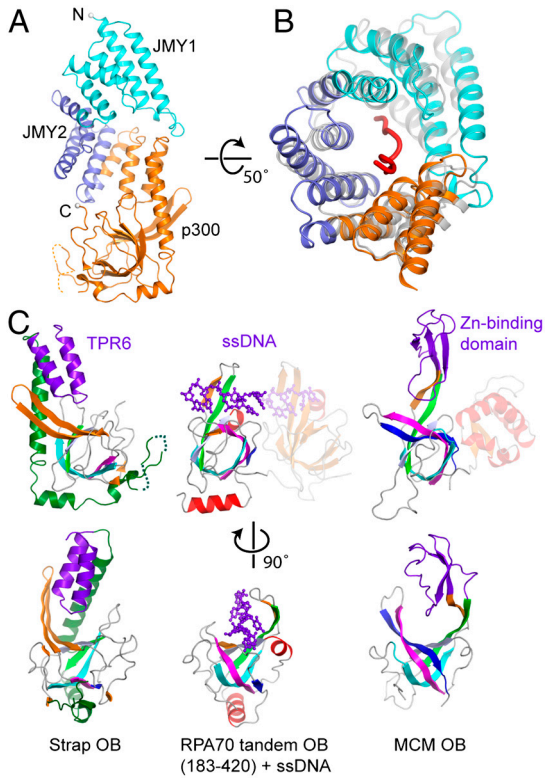

Fig. 2. Comparison of Strap with known TPR and OB-fold structures. (*A*) Strap is shown in the same orientation as the surface representation in Fig. 1*C* and is colored according to mapped interaction sites for JMY and p300. (*B*) Superposition of the Strap TPR domain and the complex of the APC6 TPR (gray) bound to a CDC26 peptide (red). Strap is viewed looking down the TPR channel from the OB-fold which is omitted for clarity. (*C*) The OB domain of Strap is compared to the structures of RPA70 (PDB: 1JMC; Dali Z-score 7.7) and the MCM complex (PDB: 1LTL; Dali Z-score 9.8). The five β-strands making up the OB-fold (β1-β5) are colored cyan, green, light blue, magenta, and dark blue, respectively. For clarity, the additional domains that pack against the RPA70 and MCM OB-folds are shown in semitransparent representation and omitted in the perpendicular view below. Strap TPR6 (purple) is tightly associated with the β2-β3 face of the OB domain as well as the β4 hairpin insert (*Left*). This occludes the region of the OB-fold typically associated with ligand binding. In the MCM complex the canonical binding surface is similarly occupied by an intramolecular protein-protein interaction with the MCM Zn-binding motif (purple, *Right*).

bacterial expression. Perhaps as a result of altered protein stability, the protein was not solubly expressed. However, evidence for flexibility at this region was provided by comparison of the two Strap molecules present in the asymmetric unit of the crystal. TPR1-5 which bind JMY were rotated 10° about the long axis of TPR6 resulting in lateral shifts of 4–7 Å (Fig. S1*C*), whereas the TPR6-OB subdomains formed a rigid unit. In solution limited tryptic digestion of wild-type Strap also identified several protease-resistant species, including a TPR6-OB fragment, demonstrating that this structural region can become accessible in solution (Fig. S5).

Following the identification of stable fragments of Strap, we cloned a series of smaller constructs of murine as well as human Strap for protein expression. Subsequently, we were able to crystallize and determine the structure of the Strap OB-fold from human. In the new structure this domain is stably folded with helices H7 and H8 and is identical to the corresponding region of the mouse structure in the full-length protein (rmsd 1.2 Å; Fig. S6). Minor differences are observed for the conformations of two loops (β4A-β4B, L12) that contact TPR6 in the full-length protein as well as loop L34 resulting from the truncated C-terminal region in the human protein used for crystallization.

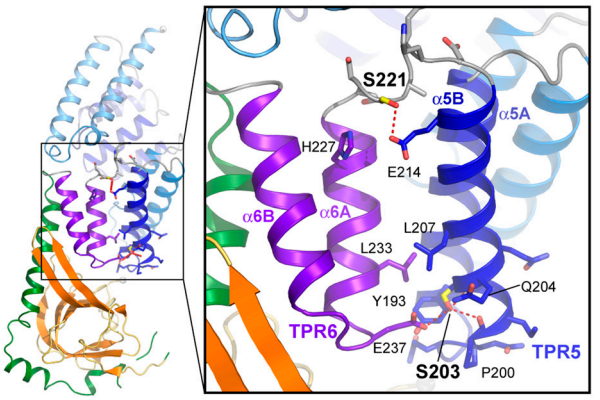

Fig. 3. Sites of Strap phosphorylation. Strap contains two reported phosphorylation sites. S203, located at the N-terminal end of α5B of TPR5, is targeted by ATM kinase and results in nuclear accumulation of Strap. This serine is completely buried in the structure and hydrogen bonds to E237 (α6A). S221, located in a 3_{10} helix (α11) between TPR5 and TPR6, is phosphorylated by Chk2 and augments protein stabilization. The solvent accessible surface areas (%ASA) for S203 and S221 are 0 and 36%, respectively.

Strap is Localized to p53 Target Genes. To clarify the functional importance of the TPR and OB domains, we expressed either the N-terminal TPR motif region or C-terminal OB-fold region of Strap, and studied the role of these domains in cell-based assays that measure different facets of the p53 response. Because transcription coactivators and cofactors frequently associate with chromatin, we assessed whether Strap was present in the chromatin of p53 target genes. By chromatin immunoprecipitation (ChIP), both Strap and each of the TPR and OB domains were localized to p53 target genes (Fig. 4 and Fig. S7*A*), consistent with interaction between Strap and the p53 transcription factor complex (6, 11) (Fig. S7*A*). These results highlight the intrinsic chromatin associating activity of the isolated TPR and OB domains.

Both the TPR and OB Domains are Required for a Strap-Dependent p53 Response. We further tested the effect of the Strap TPR and OB domains on p53-dependent transcription, using conditions in which Strap can augment p53 activity (Fig. 5). Under these conditions, neither domain was able to increase p53 activity (Fig. 5 and Fig. S7 *B–D*). Rather, the TPR and to a greater extent the OB domain were able to interfere with p53 activity (Fig. 5 and Fig. S7 *B–D*), suggestive of a dominant-negative mechanism. The

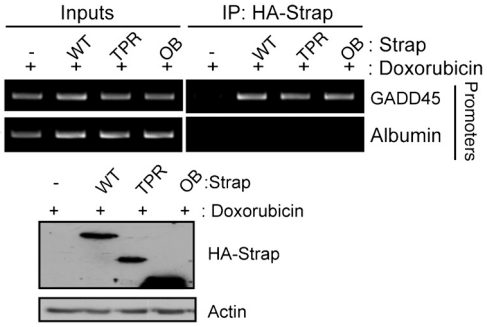

Fig. 4. Strap is present in the chromatin of p53 target genes. The ChIP assay was performed on chromatin prepared from stable U2OS cells expressing wild-type Strap, the TPR motif or OB-fold domains treated with doxorubicin (2 μM) for 6 hours. The input levels of chromatin are shown. Immunoprecipitated chromatin with anti-HA antibody was purified using Qiaquick PCR purification kit as previously described (11). The albumin gene served as a nonspecific control, and indicates vector only treated cells. GADD45 specific primers around the p53 binding site were used (11); $n = 3$. Blot represents input protein levels in the stable cell lines. Ectopic Strap was detected using the anti-HA antibody.

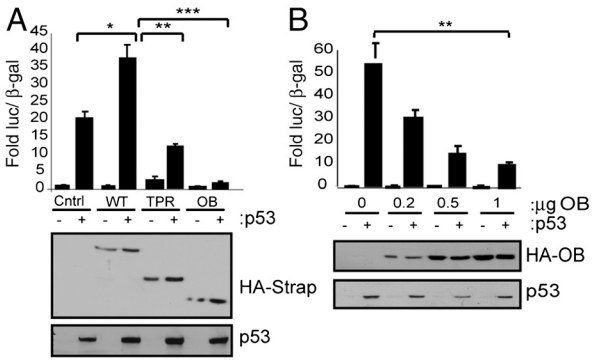

Fig. 5. The Strap TPR and OB domains show a dominant-negative effect. (*A*) Luciferase reporter assays were performed using U2OS cells transfected with expression vectors (1 μg) encoding wild-type Strap, the TPR or OB domains, and p53 as indicated and as previously described (11). The graph represents luciferase activity derived from Bax-luc (6) after normalizing for β-galactosidase activity; $n = 3$. Immunoblot represents input protein levels. (*B*) Luciferase reporter assays were performed as described in *A*, with increasing concentrations of OB-fold expression vector together with p53 as indicated. The graph represents luciferase activity after normalizing for β-galactosidase; $n = 3$. Immunoblot represents input protein levels.

inhibitory effect was evident for both domains (under equivalent nuclear localization conditions; Fig. S7*E*), and exhibited a level-dependent inhibition of p53 activity (Fig. 5*B* and Fig. S7 *C* and *D*). These results suggest that both the TPR and OB domain are functionally important in mediating the transcription cofactor effects of Strap.

To assess the role of the TPR and OB domains in the cellular stress response, we analyzed in real time U2OS and SAOS2 cells stably expressing Strap after DNA damage. In unperturbed U2OS cells, which express wild-type p53, the growth properties for wild-type Strap, TPR, and OB domain expressing cell lines were similar (Fig. 6*A*). Interestingly, a sharp increase in the number of viable adherent cells (represented by cell index) was apparent in wild-type Strap expressing cells upon DNA damage, which was less conspicuous in either the TPR or OB domain stable cells (Fig. 6 *A* and *B*). These results suggest that wild-type Strap allows more cells to survive in response to DNA damage, and further that both domains are required to effect this response. Thereafter, the precipitous decline in cell number that was evident with wild-type Strap (Fig. 6 *A* and *B*) more than likely reflects a stronger checkpoint response to DNA damage (8). Since this effect was lost in the TPR and OB domain stable cells, both domains are required for Strap to function in checkpoint control.

In a parallel study performed in SAOS2 cells (expressing a nonfunctional mutant derivative of p53), the expression of Strap hardly affected cell viability relative to the control cells under DNA damage (Fig. 6 *C* and *D*). This situation contrasted with the effect of the OB domain, where there was an increase in cell index (Fig. 6 *C* and *D*). The reduced effect of wild-type Strap in SAOS2 cells under DNA damage compared to U2OS cells is consistent with a role for p53 in mediating the effects of Strap. However, the results also suggest an additional function for the OB domain, which occurs in a fashion that is independent of p53, in the checkpoint response.

Discussion

The structure of Strap represents a substantial revision to published models of domain organization (6, 18), with new structural motifs identified throughout the protein, including the atypical TPR1 and TPR4 motifs as well as the C-terminal OB domain. The presence of two distinct domains provides a mechanism for Strap to mediate intermolecular interactions with both protein and DNA as well as a regulatory mechanism for phosphorylation.

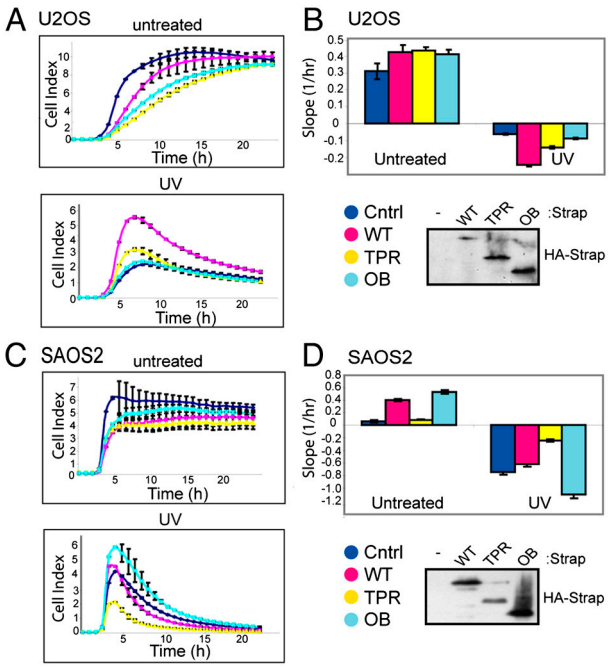

Fig. 6. Functional characterization of Strap TPR and OB domains. (*A*) U2OS cells stably expressing wild-type Strap (magenta), the TPR (yellow) or OB domains (light blue), or control (dark blue) were untreated or treated with UV (50 J/m^2) as indicated. Cells were then plated 5,000 cells/well into E-plate 16 and analyzed using a xCELLigence RTCA DP instrument. (*B*) Following the continuous xCELLigence cell monitoring in *A*, the slope (which represents the rate of change of the cell index) was calculated from time 7–20 h (i.e., when changes in cell viability were apparent) and presented graphically. The levels of Strap proteins are shown by immunoblot. (*C*) SAOS2 cells stably expressing wild-type Strap (magenta), the TPR motif (yellow) or OB-fold domains (light blue), or control (dark blue) were treated similarly to *A* and analyzed using a xCELLigence RTCA DP instrument. (*D*) The slope from *C* was calculated as in *B*.

Our structure corresponds to the unphosphorylated cytoplasmic form of Strap (Fig. 7). In this form, Strap adopts a closed conformation of both the TPR and OB domains, consistent with its cellular inactivity (6). Although the target sites for phosphorylation (7, 8) map to the outer convex face of TPRs 5 and 6, they remain largely inaccessible to protein kinases. Jiménez et al. have reported that some 15% of the annotated phosphosites in the Protein Data Bank (PDB) exhibited less than 10% solvent accessibility in the unmodified protein (19). In general agreement with these examples, the sites in Strap occur close to helix termini as well the TPR domain boundary. These positions may be more favorable for local protein unfolding, perhaps coupled to chaper-

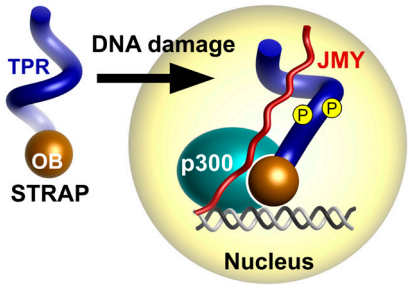

Fig. 7. Cartoon for Strap assembly with JMY and p300. Upon DNA damage Strap is phosphorylated by ATM and Chk2 kinases leading to its nuclear accumulation. Phosphorylated Strap adopts a more open and accessible conformation facilitating the assembly of the TPR and OB domains with JMY and p300, respectively. The coactivator complex is recruited to the promoters of p53 target genes and facilitates the p53 response.

one-assisted nuclear transport, to enable kinase interaction. Domain movements are also supported by our limited proteolysis. Once phosphorylated in DNA-damaged cells, steric constraints would prevent the same TPR packing, potentially leading to a more open structure for protein assembly (Fig. 7).

The OB-fold is a common feature among proteins involved in the DNA damage response and functions widely in DNA binding and protein complex assembly (20). Our data show that deletion of the OB-fold does not impair the chromatin associating activity of Strap, suggesting that the TPR domain is sufficient for assembly into some transcriptional complexes. However, deletion of the OB-fold was sufficient to impair the p53-checkpoint, underlining the importance of its binding to p300. Interestingly, a positive effect of OB-fold expression was observed in p53-null SAOS2 cells, consistent with Strap involvement in other pathways (12, 18). Strap is known to be required for survival under heat shock and functions to assemble the complex between p300 and heat shock factor 1 (HSF1) (12). In addition, Strap exhibits stress-dependent regulation of the glucocorticoid receptor (GR) that also appears dependent on both the Strap N- and C-terminal domains (18). Since p300 is known to be involved in the activity of many transcription factors, it is possible that additional Strap interaction partners remain to be identified.

The p53 response is a multifaceted signal cascade culminating in diverse cellular outcomes (2). The unpredicted domain organization and structure embodied within Strap highlights the complexity that impacts on p53 control (21). Under stress conditions, Strap is localized to p53 target genes and assembles the rich repertoire of coactivators and cofactors that influence p53 activity (Fig. 7). Both the TPR and OB domains possess intrinsic regulatory activity and are critically required for an efficient p53 response. As such, the structural and functional characterization of Strap provides new information and hints toward hitherto unexpected levels of control in the p53 response.

Materials and Methods

Protein Expression & Purification. Full-length murine Strap (Swiss-Prot Q99LG4; TTC5 residues 1–440) was subcloned as a BamHI-XhoI fragment into the vector pET28a. Human Strap (Swiss-Prot Q8N0Z6; TTC5 residues 261–424) was inserted into pNIC28-Bsa4 using ligation-independent cloning. Protein was expressed in BL21(DE3) cells using 0.5 mM IPTG for overnight induction at 18 °C. Cells were resuspended and lysed by sonication in binding buffer (50 mM Hepes pH 7.5, 500 mM NaCl, 5% glycerol, 5 mM imidazole) supplemented with 1 mM TCEP and 1 mM PMSF. Nucleic acid was removed by precipitation with 0.15% polyethyleneimine or by passage through an initial DE-52 cation exchange column. Strap protein was purified on Nickel-Sepharose using the N-terminal hexahistidine tag and imidazole elution. Strap was purified further by size exclusion chromatography using a S200 HiLoad 16/60 column buffered in 50 mM Hepes pH 7.5, 150–250 mM NaCl, 0.5 mM TCEP. A final clean-up step was performed using a monoQ column (murine Strap) or by reverse purification on Nickel-Sepharose following tag cleavage with TEV protease (human Strap). Murine Strap samples for crystallization were concentrated to 26 mg/ml buffered in 50 mM Hepes pH 7.5, 400 mM NaCl, 50 mM L-arginine, 50 mM L-glutamate, 10 mM DTT. Selenomethionine-labeled protein was expressed and purified similarly substituting selenomethionine expression media (Molecular Dimensions) for Luria broth (LB). The final sample was concentrated to 18 mg/mL. Human Strap was concentrated to 3.5 mg/mL in 50 mM Hepes pH 7.5, 250 mM NaCl, 0.5 mM TCEP.

Crystallization. Strap proteins were crystallized using the sitting drop vapor diffusion technique at 4 °C using nanolitre-sized drops. *Murine Strap*: Rod-shaped crystals of native Strap protein appeared in a number of conditions. The best crystals were grown in a 150 nL drop containing equal volumes of protein (26 mg/mL) mixed with well solution (25% tert-butanol, 0.1 M Tris pH 8.5). These crystals were monoclinic and contained two molecules per asymmetric unit (ASU) based on Matthews' coefficient. Monoclinic crystals were also grown for selenomethionine-substituted protein in drops containing 100 nL protein (18 mg/mL) mixed with 50 nL reservoir solution (10% isopropanol, 20% PEG4000, 0.1 M Hepes pH 7.5). *Human Strap*: Clusters of thin needles grew from a number of PEG/salt-containing conditions. The best crystals were grown from drops containing equal volumes of protein (3.5 mg/mL) and reservoir solution containing 36 μl of 0.2 M sodium iodide, 20% PEG3350, 10% ethylene glycol mixed with 4 μL of 0.2 M sodium acetate, 20% PEG3350, 10% ethylene glycol, 0.1 M bis-tris propane pH 8.5. Crystals belonged to space group $P2_12_12_1$ and contained a single molecule per ASU. All crystals were vitrified in well solution supplemented with 25–30% ethylene glycol.

Data Collection. Diffraction data were collected on beamline X10SA at the Swiss Light Source (Paul Scherrer Institut, Villigen, Switzerland). Data were collected from crystals at 100 K and diffraction images were recorded on a MARCCD 225 detector. *Murine Strap*: Native data were collected to a resolution of 2.05 Å. For phasing, a Se-SAD dataset was collected at a wavelength of 0.9789 Å. *Human Strap*: Native data were collected to a resolution of 1.8 Å. All data were processed with MOSFLM (22) and SCALA (23) from the CCP4 suite of programs (24).

Structure Solution and Refinement. *Murine strap*: Strap was phased using SAD data collected at the selenomethionine peak ($\lambda = 0.9789$ Å). Eighteen out of a total of 28 expected selenium sites in the asymmetric unit were located using SHELXD (25). Initial phases were calculated using SHELXE (25) and improved significantly by twofold averaging using DM (24). An initial ARP-wARP model was completed using iterative cycles of manual rebuilding in COOT (26) combined with refinement using REFMAC (27) with appropriate NCS restraints. The final model comprises two protein chains (A: 6–430; B: 1–429) encompassing the entire protein apart from residues 302–313 in a region which is poorly ordered and is only partially modeled in each chain. *Human strap*: The structure of the C-terminal domain of human STRAP was determined by molecular replacement using the corresponding domain from the mouse structure as a search model in PHASER. The final model comprises all residues (261–424) apart from a short loop (311–314). Data collection, refinement and structure quality statistics are given in Table S1.

Plasmids and Reagents. The following plasmids were used; pCMV-HA-WT Strap, pCMV-HA-Strap 200–440 (OB), pCMV-HA-p53 (6). pcDNA3 (Invitrogen), pCMV-β-galactosidase (28), pLuc-Bax (29), and pLuc-Gadd45 (30). The Strap mutant derivative pCMV-HA-Strap (1–269) (TPR) was created using oligonucleotides designed in accordance with Stratagene's QuikChange® Multi Site-Directed Mutagenesis kit using the following primer: TPR; 5′-GAA CAG CAA CTC TTG GAA TAG CTC AGT AGG CTA ACC AGC C. Cells were damaged where indicated, with 10 μM etoposide, 2 μM doxorubicin (Sigma-Aldrich) or 50 J/m^2 UV and harvested 2–16 h later. The proteasomal inhibitor Z-Leu-Leu-Leu-al (MG132) (Sigma-Aldrich) was used at concentration of 10 μM for 5 h.

Cell culture and Transfection. U2OS and SAOS2 cells were grown in DMEM (Lonza) with 5–10% fetal calf serum (FCS) in the presence of 5% (v/v) penicillin and streptomycin (Invitrogen). Cells were transfected with 100 ng of plasmid, unless indicated otherwise, using GeneJuice (Novagen) according to manufacturer's instructions.

Antibodies and Immunostaining. The following antibodies were used; mouse anti-HA HA11 (Covance) and mouse anti-p53 DO-1. For secondary antibodies, horse radish peroxidase-conjugated (Calbiochem, DAKO) antiimmunoglobulin was used. Immunostaining and immunoprecipitations were performed as previously described (7). Chromatin immunoprecipitations were performed as described (31). The primers used were as follows: Bax; Fwd 5′-TAA TCC CAG CGC TTT GGA AGG, Rev 5′-TGC AGA GAC CTG GAT CTA GCA A, Gadd45; Fwd 5′-GGA TCT GTG GTA GGT GAG GGT CAG G, Rev 5′-GGA ATT AGT CAC GGG AGG AGG CAG TG, Albumin; Fwd 5′-TGG GGT TGA CAG AAG AGA AAA GC, Rev 5′-TAC ATT GAC AAG GTC TTG TGG AG (11, 31).

Reporter Assay. Reporter assay was performed as described previously (31).

xCELLigence. 5,000 cells/well into E-plate 16. Experiments were carried out using the RTCA DP instrument (Roche Diagnostic GmbH, Germany) which was placed in a humidified incubator maintained at 37 °C with 5% CO_2. The electronic sensors provided a continuous and quantitative measurement of cell index in each well. Cell index is a quantitative measure of cell number present in a well e.g. lower cell index reflects fewer cells are attached to the electrodes. The E-Plate 16 was monitored over the time frame indicated.

Accession Codes. Protein Data Bank: coordinates and structure factors have been deposited with accession codes 4ABN (full-length murine Strap) and 2XVS (human Strap OB-fold).

ACKNOWLEDGMENTS. We thank the Medical Research Council, Cancer Research UK (CRUK), Leukemia Research Fund (LRF), Association for Interna-

tional Cancer Research (AICR), and European Union (EU) for supporting this work, and Rosemary Williams for help in preparing this manuscript. We thank Oleg Fedorov and Structural Genomics Consortium staff for help with the Octet Optical Biosensor. The Structural Genomics Consortium is a registered charity (number 1097737) that receives funds from the Canadian Institutes for Health Research, the Canadian Foundation for Innovation, Genome Canada through the Ontario Genomics Institute, GlaxoSmithKline, Karolinska Institutet, the Knut and Alice Wallenberg Foundation, the Ontario Innovation Trust, the Ontario Ministry for Research and Innovation, Merck & Co., Inc., the Novartis Research Foundation, the Swedish Agency for Innovation Systems, the Swedish Foundation for Strategic Research, and the Wellcome Trust.

1. Levine AJ, Oren M (2009) The first 30 years of p53: Growing ever more complex. *Nat Rev Cancer* 9:749–758.
2. Murray-Zmijewski F, Slee EA, Lu X (2008) A complex barcode underlies the heterogeneous response of p53 to stress. *Nat Rev Mol Cell Biol* 9:702–712.
3. Brooks CL, Gu W (2006) p53 ubiquitination: Mdm2 and beyond. *Mol Cell* 21:307–315.
4. Brown CJ, Lain S, Verma CS, Fersht AR, Lane DP (2009) Awakening guardian angels: Drugging the p53 pathway. *Nat Rev Cancer* 9:862–873.
5. Vousden KH, Prives C (2009) Blinded by the light: The growing complexity of p53. *Cell* 137(3):413–431.
6. Demonacos C, Krstic-Demonacos M, La Thangue NB (2001) A TPR motif cofactor contributes to p300 activity in the p53 response. *Mol Cell* 8:71–84.
7. Demonacos C, et al. (2004) A new effector pathway links ATM kinase with the DNA damage response. *Nat Cell Biol* 6:968–976.
8. Adams CJ, et al. (2008) ATM and Chk2 kinase target the p53 cofactor Strap. *EMBO Rep* 9:1222–1229.
9. Shikama N, et al. (1999) A novel cofactor for p300 that regulates the p53 response. *Mol Cell* 4:365–376.
10. Coutts AS, Weston L, La Thangue NB (2009) A transcription co-factor integrates cell adhesion and motility with the p53 response. *Proc Natl Acad Sci USA* 106:19872–7.
11. Jansson M, et al. (2008) Arginine methylation regulates the p53 response. *Nat Cell Biol* 10:1431–1439.
12. Xu D, Zalmas LP, La Thangue NB (2008) A transcription cofactor required for the heat-shock response. *EMBO Rep* 9:662–669.
13. D'Andrea LD, Regan L (2003) TPR proteins: The versatile helix. *Trends Biochem Sci* 28:655–662.
14. Wang J, Dye BT, Rajashankar KR, Kurinov I, Schulman BA (2009) Insights into anaphase promoting complex TPR subdomain assembly from a CDC26-APC6 structure. *Nat Struct Mol Biol* 16:987–989.
15. Holm L, Rosenstrom P (2010) Dali server: Conservation mapping in 3D. *Nucleic Acids Res* 38(Suppl):W545–549.
16. Arcus V (2002) OB-fold domains: a snapshot of the evolution of sequence, structure and function. *Curr Opin Struct Biol* 12:794–801.
17. Fletcher RJ, et al. (2003) The structure and function of MCM from archaeal M. Thermoautotrophicum. *Nat Struct Biol* 10:160–167.
18. Davies L, et al. (2011) Regulation of glucocorticoid receptor activity by a stress responsive transcriptional cofactor. *Mol Endocrinol* 25:58–71.
19. Jimenez JL, Hegemann B, Hutchins JR, Peters JM, Durbin R (2007) A systematic comparative and structural analysis of protein phosphorylation sites based on the mtcPTM database. *Genome biology* 8:R90.
20. Flynn RL, Zou L (2010) Oligonucleotide/oligosaccharide-binding fold proteins: A growing family of genome guardians. *Crit Rev Biochem Mol Biol* 45:266–275.
21. Coutts AS, La Thangue NB (2005) The p53 response: Emerging levels of co-factor complexity. *Biochem Biophys Res Commun* 331:778–785.
22. Leslie AGW (2006) The integration of macromolecular diffraction data. *Acta Crystallogr D Biol Crystallogr* 62:48–57.
23. Evans P (2006) Scaling and assessment of data quality. *Acta Crystallogr D Biol Crystallogr* 62:72–82.
24. Collaborative Computational Project Number 4 (1994) The CCP4 Suite—Programs for protein crystallography. *Acta Crystallogr D Biol Crystallogr*, 50 pp:760–763.
25. Sheldrick GM (2008) A short history of SHELX. *Acta Crystallogr A* 64:112–122.
26. Emsley P, Lohkamp B, Scott WG, Cowtan K (2010) Features and development of Coot. *Acta Crystallogr D Biol Crystallogr* 66:486–501.
27. Murshudov GN, Vagin AA, Dodson EJ (1997) Refinement of macromolecular structures by the maximum-likelihood method. *Acta Crystallogr D Biol Crystallogr* 53:240–255.
28. Milton AH, Khaire N, Ingram L, O'Donnell AJ, La Thangue NB (2006) 14-3-3 proteins integrate E2F activity with the DNA damage response. *EMBO J* 25:1046–1057.
29. Miyashita T, Reed JC (1995) Tumor suppressor p53 is a direct transcriptional activator of the human bax gene. *Cell* 80:293–299.
30. Kastan MB, et al. (1992) A mammalian cell cycle checkpoint pathway utilizing p53 and GADD45 is defective in ataxia-telangiectasia. *Cell* 71:587–597.
31. Zalmas LP, et al. (2008) DNA-damage response control of E2F7 and E2F8. *EMBO Rep* 9:252–259.